Journal of Sustainable Metallurgy (2024) 10:687–698
https://doi.org/10.1007/s40831-024-00817-2

RESEARCH ARTICLE

Silane Gas Production Through Hydrolysis of Magnesium Silicide by Hydrochloric Acid

Azam Rasouli[1] · Raphael Kuhn[2] · Samson Yuxiu Lai[2] · Jafar Safarian[1] · Gabriella Tranell[1]

Received: 17 December 2023 / Accepted: 17 March 2024 / Published online: 17 April 2024

Abstract

Monosilane (SiH_4) is a common precursor for the production of high-purity silicon for solar PV applications. As an alternative to carbothermic reduction of silica to produce metallurgical grade silicon with subsequent conversion to silane, an alternative route over magnesiothermic reduction of silica to Mg_2Si has been explored in our earlier work. In the current work, silane gas production through hydrolysis of Mg_2Si in HCl acid solution was studied. Two sources of Mg_2Si were chosen: a commercial Mg_2Si source and a Mg_2Si source produced through magnesiothermic reduction of high-purity natural quartz. Effects of various parameters on the hydrolysis of Mg_2Si, including different experimental setups, temperature of the acid solution, acid concentration, reaction time, and relative amounts of reactants were studied. The evolution of produced gases was determined by two different methods: firstly, by passing the produced gas through a KOH solution to capture Si with subsequent analysis of the Si content in the KOH solution by inductively coupled plasma mass spectrometry and secondly, on-line gas analysis by GC–MS. The silane distribution between different silane species with reaction time was evaluated and the activation energy of silane formation was calculated. The results indicated comparable silane yields obtained from the on-line GC–MS method and KOH solution analysis method, as well as for commercial Mg_2Si and the Mg_2Si–MgO mixture produced through magnesiothermic reduction. Furthermore, adding HCl acid to Mg_2Si in water led to higher SiH_4 formation yield than adding Mg_2Si to acid. However, the total silane yield for the two methods was similar at approximately 32%.

The contributing editor for this article was U. Pal.

✉ Azam Rasouli
azam.rasouli@ntnu.no

[1] Department of Materials Science and Engineering, Norwegian University of Science and Technology, Trondheim, Norway

[2] Battery Technology Department, Institute for Energy Technology (IFE), Kjeller, Norway

Graphical Abstract

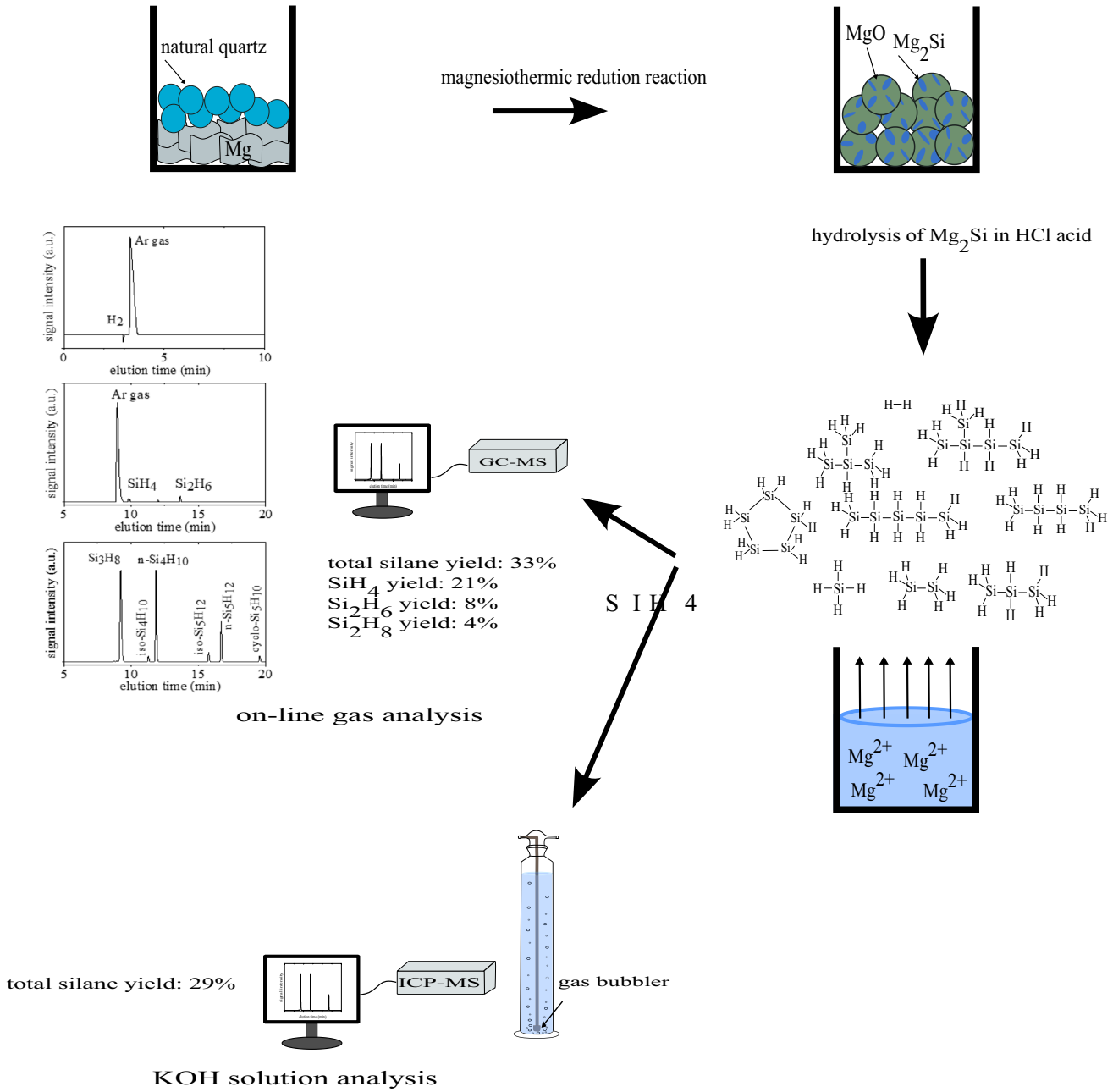

Keywords Silane formation · Hydrolysis of Mg_2Si · Silane yield · Silane distribution

Introduction

Further development of solar energy conversion technologies and materials is vital to reduce CO_2 emissions from electricity generation. Currently, solar energy accounts for 5% of global electricity generation but it is predicted that the sector will experience rapid growth in the years to come and play a significant role in electricity generation by 2027 [1]. With the rapid growth of solar PV, CO_2 emissions from solar cell and component production also increase. High-purity silicon (polysilicon with a purity of 9N) is responsible for a large part of CO_2 emissions in the Si-based solar module production process, accounting for over 39%. Therefore, lowering the carbon footprint of the polysilicon production process is necessary to reduce total CO_2 emissions [1–3].

Carbothermic reduction of SiO_2 to obtain metallurgical grade silicon as a precursor to polysilicon is responsible for approximately 5 kg CO_2 eq/kg silicon in direct (scope 1) emissions, not including energy production (scope 2) emissions. Typically, high-purity gaseous $HSiCl_3$ or SiH_4 intermediates are produced from metallurgical grade silicon and subsequently decomposed at high temperature to polysilicon. SiH_4 is decomposed at a temperature range of 680–800 °C, while decomposition of $HSiCl_3$ takes place between 850 and 1200 °C. Decomposition of SiH_4 offers the advantage of lower energy consumption and elimination of corrosive and toxic gases compared to the decomposition of $HSiCl_3$. However, the latter technology is still the main process to produce polysilicon as most factories have already been built based on the production and decomposition of $HSiCl_3$. It is predicted that the share of polysilicon production using SiH_4 in the fluidized bed reactor will increase with the rapid growth of PV modules [2, 4–7].

SiH_4 may be produced through different chemical reactions and processes, with their respective advantages and disadvantages, as listed in Table 1. Among these, the Union Carbide method has been used as the main industrial production process for SiH_4, despite its relatively high energy consumption and associated formation of $SiCl_4$ as by-product [7–12]. Production of SiH_4 by HCl acid hydrolysis of magnesium silicide is considered an attractive process in terms of simplicity and reduced CO_2 emissions. The low silane yield has, however, hindered its further development [13–19]. In the present study, SiH_4 gas production through hydrolysis of both pure Mg_2Si and Mg_2Si produced by magnesiothermic reduction of quartz has been further investigated with the aim of improving the production yield of SiH_4 gas and comparing the production yield using two Mg_2Si sources. Various silicide compounds, such as Mg_2Si, Ca_2Si, and ternary alloys such as Al–Ca–Si react with an acid solution to produce silane gases. In this study, Mg_2Si was chosen because Mg as an element is safer to work with, and previous studies have not shown significant silane yield formation when other silicides were used [15, 24, 25]. The gas evolution during the progress of reaction was simultaneously measured using GC–MS. Furthermore, the effects of different parameters on silane yield have been studied,

Table 1 Different methods of silane production

Method	Chemical reaction		Comments
Lithium aluminum hydride method [20, 21]	$SiCl_4 + 4LiAlH_4 \rightarrow LiCl + AlCl_3 + SiH_4$	Equation 1	Conducted at RT up to 65 °C, uses tetrahydrofuran as the solvent Advantage: high silane yield Disadvantage: the high cost and introduction of carbon to the produced silane by degradation of the solvent
Lithium hydride method [21, 22]	$SiCl_4 + 4LiH \rightarrow 4LiCl + SiH_4$	Equation 2	Conducted in a molten salt (375–425 °C) Advantage: high silane yield Disadvantage: high electrical energy consumption and difficulties in handling molten salt
Magnesium silicide method [13, 14, 23]	$Mg_2Si + 4HCl \rightarrow SiH_4 + MgCl_2$	Equation 3	Conducted at RT up to 65 °C Advantage: simple method with low energy consumption Disadvantage: low silane yield
	$Mg_2Si + 4NH_4Br \rightarrow SiH_4 + 2MgBr_2 + 4NH_3$	Equation 4	Conducted at − 33 °C or at RT and high pressure Advantage: high silane yield Disadvantage: low temperature, low solubility of $MgBr_2$ in the ammonium solution, contamination of product by ammonia
Union carbide method [7, 8, 10]	$5Si + 16HCl \rightarrow 4SiHCl_3 + 6H_2 + SiCl_4$ $3SiCl4 + Si + 2H_2 \rightarrow 4HSiCl_3$ $4HSiCl_3 \rightarrow SiH_4 + 3SiCl_4$	Equation 5 Equation 6 Equation 7	$SiHCl_3$ is produced at 250–300 °C in a fluidized bed reactor and then converted to SiH_4 through a series of disproportionation reactions Advantage: high silane yield by $SiCl_4$ recovery Disadvantage: requirement to use corrosion resistant material, formation of high amount of $SiCl_4$ that leads to low silane yield

including acid concentration, acid volume-to-alloy weight ratio, temperature, alloy preparation temperature, as well as the order of reactant mixing.

Experimental Procedure

Materials

Two Mg_2Si sources were selected to carry out silane gas production experiments. The first source was a commercial Mg_2Si (99.99%, 3–12 mm pieces, supplied by Alfa Aesar) and the other source was the product from magnesiothermic reduction of natural quartz at three different temperatures (800, 900, and 1100 °C). The details of the experimental method to magnesiothermically prepare Mg_2Si are described in our previous publications [26, 27]. Mg_2Si from both sources were ball-milled to obtain powder with a particle size of below 40 µm.

Hydrolysis of Mg_2Si

To carry out the reaction between Mg_2Si and HCl acid solution, a custom designed glass reactor was made, as depicted in Fig. 1. This reactor allowed for the charging of either Mg_2Si in the dropping funnel and acid solution in the round-bottom flask (setup 1) or acid solution in the dropping funnel and Mg_2Si and water in the round-bottom flask (setup 2). Prior to and during charging of reactants, the reactor was purged with Ar gas. The reaction was initiated by mixing Mg_2Si and acid solution in the round-bottom flask by either setup 1 or setup 2, using a magnetic stirrer with a rotation speed of 200 rpm. To conduct the reaction at the desired temperature, the round-bottom flask was placed in a water bath on a hot plate (Fig. 1). Table 2 lists the various parameters studied to conduct the reaction between Mg_2Si and the aqueous acid solution.

Characterization

Two methods were employed for analyzing the produced gas. With the first method, the produced gas was passed through an aqueous KOH solution using a gas frit with relatively small pores (size of 1–1.7 µm). With this method, produced silane gas reacts with the KOH solution to form K_2SiO_3. For example, SiH_4 and Si_2H_6 silanes react with KOH according to Eqs. 8 and 9, respectively. Higher silanes react with the KOH solution in a similar way to SiH_4 and Si_2H_6 [28]. Subsequently, silane yields from Mg_2Si hydrolysis were calculated by measuring the total Si content of the KOH solution by inductively coupled plasma mass spectrometry. The inductively coupled plasma mass spectrometry analysis was performed using an Agilent 8900 Triple Quadrupole inductively coupled plasma mass spectrometry (ICP-QQQ) instrument with SPS 4 Autosampler. The blank KOH solution sample had a Si content of less than 1 ppm,

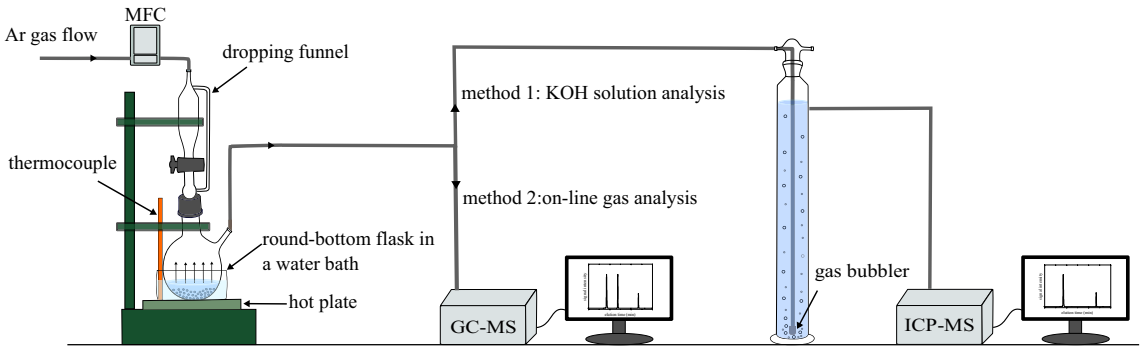

Fig. 1 The schematic of the experimental setup and analysis methods used to study the reaction between Mg_2Si and HCl acid solution

Table 2 Selected parameters of silane gas production experiments

Parameters	Values
Mg_2Si source	Commercial Mg_2Si, mixture of Mg_2Si with either Si or Mg, Mg_2Si produced through magnesiothermic reduction
Temperature (°C)	20–60
HCl acid solution concentration (w/w)	8–20
Mg_2Si (mg)	300–1200
Reaction time (min)	1–40

indicating the measured Si in the solution after conducting hydrolysis reaction was related to the silane reaction with the KOH solution. The silane yield using the KOH method was obtained using Eq. 10.

$$SiH_4 + 2KOH + H_2O \rightarrow K_2SiO_3 + 4H_2 \Delta G_{30°C} = -531kJ \quad (8)$$

$$Si_2H_6 + 4KOH + 2H_2O \rightarrow 2K_2SiO_3 + 7H_2 \Delta G_{30°C} = -1075kJ \quad (9)$$

$$\text{Silane yield}(\%) = \frac{\text{Sicontent of KOH(mg)}}{\text{total Si in}Mg_2Si\text{(mg)}} \times 100 \quad (10)$$

With the second method, the produced gas was analyzed on-line using a specially designed Agilent 7890B Gas Chromatography (GC) instrument. The instrument was equipped with three detectors including a thermal conductivity detector (TCD_{perm}) for detecting inert gases (permanent gases) like Ar, H_2, N_2, and He; a TCD_{silane} for detecting SiH_4 and Si_2H_6 gases; and the MSD (Quadrupole Mass Selective Detector) for detecting higher silanes. An over-pressure of 1.3 bar was used to have a suitable flow of gas from the glass reactor to the GC–MS. Detailed information about the GC–MS analysis can be found in an earlier publication by Wyller et al. [29]. The elution times and concentrations of SiH_4, Si_2H_6, and Si_3H_8 were determined by utilizing calibration standard silane gases. The composition of the calibration standard silane gases, as well as the calibration graphs, are presented in the online supplementary Table S-1 and online supplementary Fig. S-1, respectively (refer to electronic supplementary material). The first method of analyzing the produced gas (KOH solution method) was used to obtain silane yield, while concentrations and distributions of silane types in addition to silane yield were obtained using the second method (GC–MS method).

After the hydrolysis experiments, the HCl acid solution was filtered to collect the solid residue in the solution. The collected residues were dried for 24 h at 100 °C. The initial Mg_2Si sources and the residues in the acid solution were subjected to X-ray diffraction analysis using a Bruker D8 Focus instrument. The phases of the obtained XRD patterns were identified by the DIFFRAC.EVA V6.0 software, using the PDF-4+2014 database.

Results and Discussion

The Solid Materials Analysis

Figure 2 displays the XRD patterns of the commercial Mg_2Si and Mg_2Si produced through magnesiothermic reduction of quartz at 800, 900, and 1100 °C, denoted MR-800, MR-900, and MR-1100, respectively. The commercial sample primarily consisted of Mg_2Si with a small quantity of Si. The

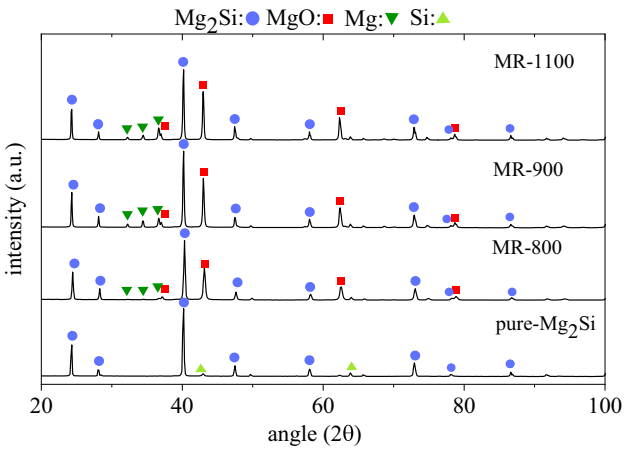

Fig. 2 X-ray diffraction patterns of different Mg_2Si sources

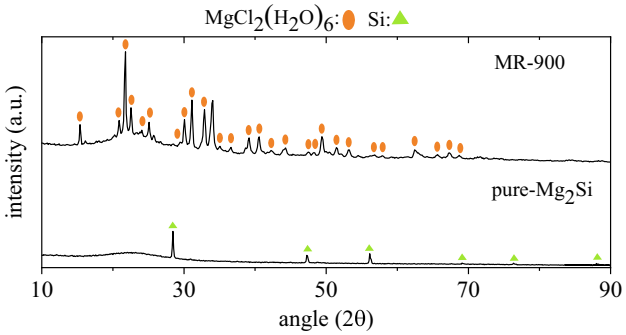

Fig. 3 X-ray diffraction patterns of residues in acid solutions post reaction

Mg_2Si produced via magnesiothermic reduction consisted of Mg_2Si and MgO as the primary phases, with a small amount of Mg present. MgO is the by-product of the magnesiothermic reduction reaction, according to Eq. 11.

Figure 3 illustrates the X-Ray Diffraction (XRD) patterns of the solid residues after the reaction with HCl solution. It is apparent that there were no residual Mg_2Si peaks in the spectrum obtained from the residues. In the residue from commercial Mg_2Si, small Si peaks together with the broad peak at 22° associated with the amorphous phase of SiO_2 were found. The inductively coupled plasma mass spectrometry analysis revealed that all the Mg was in the acid solution after commercial Mg_2Si hydrolysis reaction. For the MR-900 residue sample, the primary phase was $MgCl_2(H_2O)_6$, a solid compound in the $MgCl_2$–HCl–H_2O system in addition to the broad SiO_2 peaks at approximately 2θ of 22°. The higher Mg content (as both Mg_2Si and MgO) of the MR-900 sample led to the formation of a supersaturated solution. The mass balance calculation using inductively coupled plasma mass spectrometry result indicated approximately 90% of Mg was in the acid solution and the rest of Mg in the residue as a

$MgCl_2(H_2O)_6$. The formation of amorphous SiO_2 will be discussed in detail later.

$$SiO_2 + 4Mg \rightarrow Mg_2Si + 2MgO \quad (11)$$

The Silane Gas Analysis

Analysis of Evolved Gases

The chromatographs obtained from the reaction of the commercial Mg_2Si sample using the on-line GC–MS are presented in Fig. 4. The chromatograph obtained from TCD_{silane}, in Fig. 4a, illustrates the presence of SiH_4 and Si_2H_6 peaks, respectively, at elution times of 9.82 min and 13.65 min. A small peak detected at the elution time of 12.01 min remains unidentified. This peak has been observed for the blank sample and may be related to water or HCl acid vapor. Figure 4b depicts the detection of higher silanes, namely Si_3H_8, Si_4H_{10}, and Si_5H_{12}, detected by MSD. The elution time of Si_3H_8 has already been established from calibration standard gases at 9.18 min. For higher silanes, Si_4H_{10} and Si_5H_{12}, no calibration standard gases were available. To investigate the presence of these gases, the selected ion monitoring mode of MSD was utilized, as shown in Fig. 5. As seen in this figure, iso-Si_4H_{10} and *n*-Si_4H_{10} isomers of tetrasilane and iso-Si_5H_{12}, *n*-Si_5H_{12} and cyclo-Si_5H_{10} isomers of pentasilane were detected [29].

The boiling points of silane gases increase with Si content of their molecule. SiH_4 and Si_2H_6 have boiling points below 0 °C, specifically − 119.5 °C and − 14.5 °C, respectively. The boiling point of Si_3H_8 is 52.9 °C, which is near the reaction temperature employed in this study [30]. Higher silane gases, including Si_4H_{10} and Si_5H_{12}, have boiling points above 100 °C [30–32]. Therefore, the detection of Si_4H_{10} and Si_5H_{12} by MSD was related to their partial evaporation. The formation of these higher silanes, up to $Si_{15}H_{32}$, in relatively low concentrations has also been reported in previous works. It should be noted that higher silanes are relatively unstable compounds that may dissociate into lower silanes, even at room temperature [13, 15, 18, 19, 33].

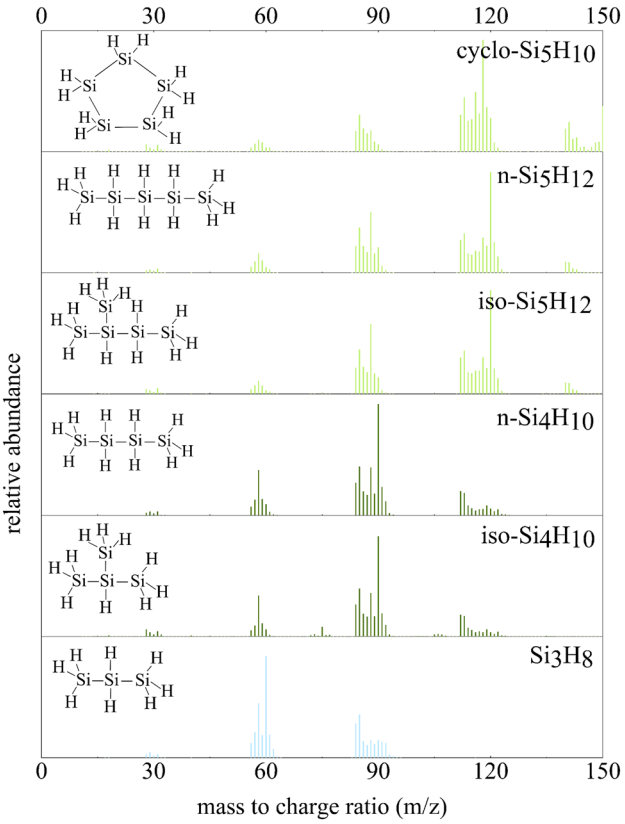

Fig. 5 The mass spectra of Si_3H_8, Si_4H_{10}, and Si_5H_{12} obtained by MSD

Concentrations of Si_4H_{10} and Si_5H_{12} could not be determined quantitatively without standards. For these silanes, it was hence presumed that their concentrations were linear functions of their peak areas. The comparison of peak areas, Fig. 4b, indicates that *n*-Si_4H_{10} and *n*-Si_5H_{12} with linear structure qualitatively had the highest concentrations among tetrasilane and pentasilane isomers. Furthermore, an H_2 peak

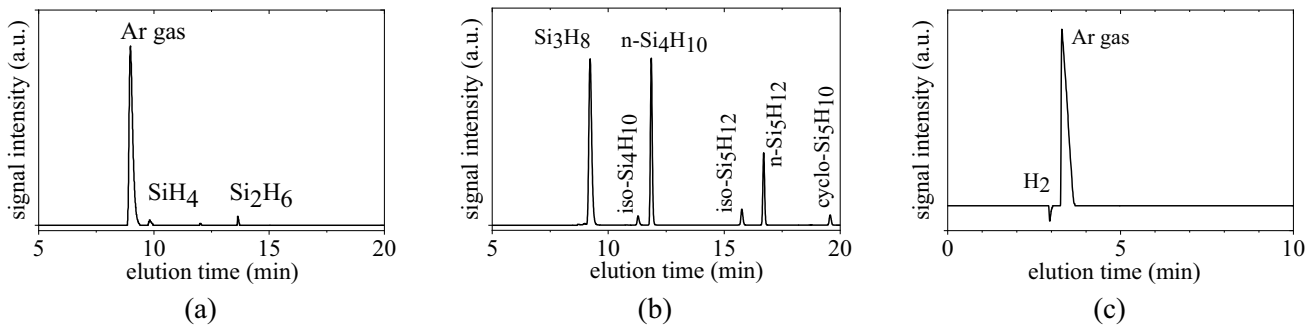

Fig. 4 Chromatographs obtained from TCD_{silane} (**a**), MSD (**b**), and TCD_{perm} (**c**)

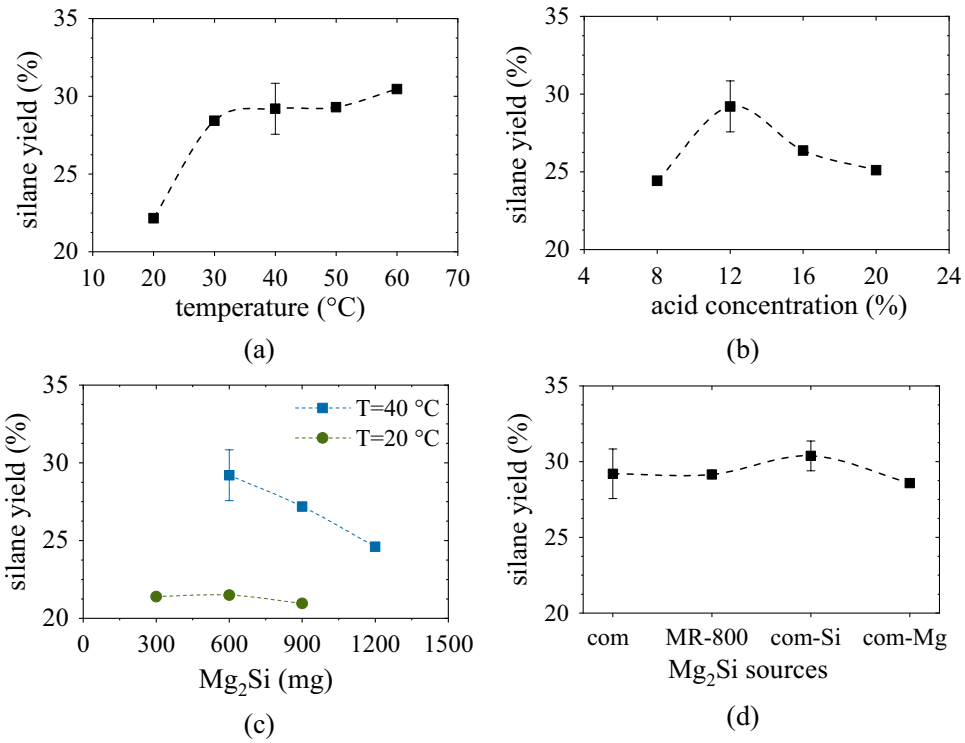

Fig. 6 Effects of temperature (**a**), acid concentration (**b**), relative amounts of reactants (**c**), and Mg_2Si sources (**d**) on the silane yield obtained by the KOH solution method (the first method)

was found in the chromatograph obtained by TCD_{perm}, as shown in Fig. 4c.

Effect of Reaction Conditions on Silane Yield Using KOH Solution Method

The effects of various reaction parameters on the silane yield, including temperature, acid concentration, relative amount of the reactants, and Mg_2Si sources are presented in Fig. 6. As seen in Fig. 6a, the silane yield increased with rising temperature from 20 to 40 °C, while further increase in temperature did not result in significant yield improvement. Figure 6b demonstrates that the highest silane yield was achieved at an acid concentration of 12%. Previous studies have suggested a temperature of 50 °C and an acid concentration of 10–12% as optimal conditions for obtaining high silane yield [15, 16]. Consequently, to investigate other reaction parameters, a temperature of 40 °C and an acid concentration of 12% were selected.

In Fig. 6c, no significant differences were observed when different amounts of Mg_2Si, from 300 to 900 mg, were added to a constant acid volume at 20 °C. However, at a temperature of 40 °C, the silane yield decreased with an increasing amount of Mg_2Si from 600 to 1200 mg with a constant acid volume of 60 ml. Additionally, various sources of Mg_2Si, including commercial Mg_2Si, Mg_2Si obtained from magnesiothermic reduction, a mixture of commercial Mg_2Si and Si (com-Si), and a mixture of commercial Mg_2Si and Mg (com-Mg) resulted in similar total silane yields of approximately 29%, shown in Fig. 6d. In the MR-800 and com-Mg samples, besides the reaction of Mg_2Si with the acid solution, MgO and Mg also reacted with HCl, as indicated by Eqs. 12 and 13, respectively. However, these reactions did not seem to affect the silane formation reactions negatively.

$$MgO_{(S)} \overset{HCl}{\rightarrow} Mg^{2+} + O^{2-} \tag{12}$$

$$Mg_{(S)} + 2H^{+} \overset{HCl}{\rightarrow} Mg^{2+} + H_{2(l)} \tag{13}$$

Effect of Reaction Conditions on Silane Yield and Silane Distribution Using GC–MS Method

The silane gas generation against reaction time using the two different setups is presented in Fig. 7a for the commercial Mg_2Si and MR-1100 samples using the GC–MS method. As seen in this figure, the production of silane gas declined rapidly with reaction time, and setup 2 generated a relatively higher quantity of silane gas initially compared to setup 1. The distribution of SiH_4, Si_2H_6, and Si_3H_8 gases, Fig. 7b, illustrates approximately constant silane distributions with time. The comparison of peak areas of *n*-Si_4H_{10} and *n*-Si_5H_{12} with time reveals a higher amount of their formation in setup 1, as shown in Fig. 7c.

The silane concentration graphs in Fig. 7a were integrated to obtain total silane yield, Si yield in different silane types,

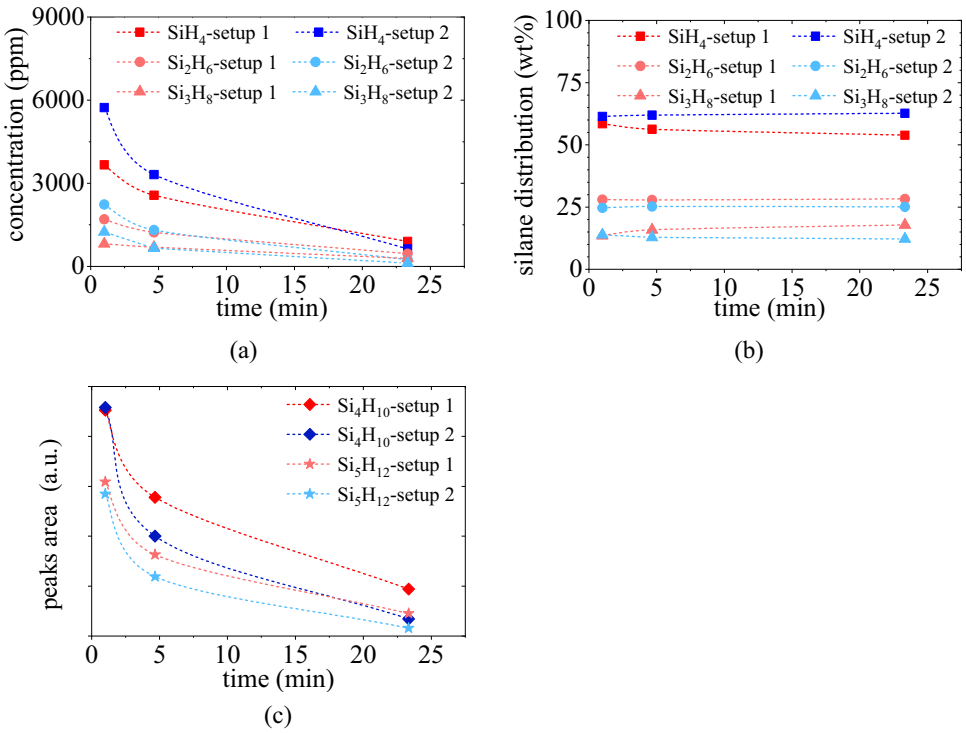

Fig. 7 The change in the concentration of SiH_4, Si_2H_6, and Si_3H_8 with reaction time for two different setups (**a**), the change in their distribution with reaction time (**b**), areas of *n*-Si_4H_{10} and *n*-Si_5H_{12} isomer peaks with reaction time (**c**), obtained by GC–MS

and their total distribution. The Si yield of each silane type is defined as the amount of Si in each silane type to the total amount of Si in Mg_2Si. As indicated in Table 3, SiH_4 yields were 18% and 21% in setup 1 and setup 2, respectively, indicating a few percent more SiH_4 formation in setup 2 than setup 1. The SiH_4 yield in the present work is hence higher than the values of 9% and ≈12% obtained by Stock and Somieski and Belot et al., respectively [13, 15].

Furthermore, the total silane yield, which is defined as the total Si in various silane types to the total amount of Si in Mg_2Si, is calculated to 32% and 33% in setup 1 and setup 2, respectively (Table 3). Previous research has shown that adding acid solution to the Mg_2Si resulted in negligible silane formation, while adding Mg_2Si powder to the acid solution resulted in a higher silane yield [15]. Consequently, most of the research employed the latter method. As seen in Table 3, by adding water to Mg_2Si, no significant difference in silane yield was measured between the two methods in this study. In a pioneer work by Stock and Somieski, 3.17 g out of total 13.7 g Si in the initial Mg_2Si reactant was converted to silane, which is equivalent to 23% silane yield [13]. In later works, silane yields of 13%, 14%, and ≈20% were reported, respectively, by Johnson and Isenberg, Nandi et al., and Belot et al. [15, 16, 34]. In the latter one, large-scale experiments were carried out in which 5.6 kg silane gas was produced using 70 kg of an alloy with a chemical composition of Al33%–Ca18%–Si40%. The produced gas was composed of 3.3 kg of SiH_4, 1 kg of Si_2H_6, and the rest was marked as higher silanes. The silane yield of 32% from the present work is somewhat higher than all mentioned works. In a recent study by Serikkanov et al., it was claimed that adding water and then concentrated acid to the Mg_2Si, as in the current study, resulted in a significantly higher silane yield of around 80% [35]. However, the method of measuring silane yield was not described.

Further experiments under different reaction conditions, including different Mg_2Si sources, setups, temperatures, and acid concentrations demonstrate similar silane distribution at the early stage of reaction times which are listed in Table 4.

The total silane yields obtained by two methods, the KOH solution method and GC–MS method, are also comparable. However, some differences need to be taken into consideration when evaluating the accuracy of the results. The total silane yield was measured over a reaction duration of 40 min using the KOH solution method, while for the experiments using the GC–MS, gas measurements were done over a duration of 20 min. The total silane yield calculated from the GC–MS method was, however, approximately 3% higher than that obtained from the KOH solution method. This discrepancy could suggest that not all the produced silane gas reacts with the KOH solution. After each experiment, the experimental setup was carefully inspected for the presence of SiO_2 white powder. The presence of such powder would indicate an undesired reaction of the produced silane with oxygen in the air instead of its intended reaction with the KOH solution. The absence of any visible white powder suggests that most of the silane had reacted with the KOH solution.

Table 3 Silane yield and distribution for the two setups obtained by GC–MS and KOH solution methods

Sample	Setup	Si yield in different silane types (%)			Total silane yield obtained from two analysis methods		Total silane distribution (wt%)		
		SiH_4	Si_2H_6	Si_3H_8	GC–MS method	KOH method	SiH_4	Si_2H_6	Si_3H_8
Commercial Mg_2Si	Setup 1	18	9	5	32	29 ± 1.6	56	28	16
MR-1100	Setup 2	21	8	4	33	29	62	25	13
Stock and Somieski [13]	–	9	7	4	19	–	45	35	20
Belot et al. [15]	–	≈12	≈4	–	16*	–	–	–	–

*The total silane in SiH_4 and Si_2H_6

However, the differences in yield are small enough to be explained by other factors, such as calibrations of GC–MS and inductively coupled plasma mass spectrometry, as well as estimations of non-calibrated measurements of higher silanes.

Reaction Mechanism and Side Reactions

Mg_2Si and HCl react according to Eq. 14 to form SiH_4 gas and simultaneously, higher silanes are formed. Equation 14 is an ideal reaction describing the complete conversion of Si in Mg_2Si to SiH_4. Under real conditions, however, another simultaneous reaction, described by Eq. 15 occurs, leading to a decrease in the silane yield. The Gibbs free energy of reactions Eqs. 14 and 15 (calculated by FactSage 8.1) shows that the formation of SiO_2 is thermodynamically more favorable than SiH_4 formation. Schwarz and Konrad and Feher and Tromm proposed the mechanism of silane formation by Mg_2Si and HCl reaction through a series of intermediate reactions [36, 37]. First, Mg_2Si is hydrolyzed in water to form a $(HOMg)_2SiH_2$ compound, Eq. 16. Then, the Cl ion breaks the Mg–Si bond in the $(HOMg)_2SiH_2$ compound, resulting in the formation of SiH_2 radicals, Eq. 17. SiH_2 radicals are polymerized in water to form $(SiH_2)_n$ chains which participate in various reactions to form different compounds such as SiO_2, H_2, SiH_4, Si_2H_6, Si_3H_8, SiH_2O, and etc. described by Eqs. 18 to 21. SiH_2O is finally converted to SiO_2 according to Eq. 22. Therefore, Si in Mg_2Si ends up either in silanes or SiO_2.

The observation of higher silanes confirms the polymerization of the Si compound, however, the formation of iso- and cyclic isomers with branched or cyclic structures was relatively low. The *n*-Si_4H_{10} and *n*-Si_5H_{12} species with linear structure were the main isomers formed. Furthermore, the high negative enthalpies of reactions defined in Eqs. 14 and 15, respectively, − 814 kJ and− 1188 kJ, indicate that the temperature can rise considerably during these reactions. A temperature increment from 50 to 75 °C was observed for a large-scale experiment, adding 70 kg of silicide alloy to 1100 l of acid with a charging rate of 8 kg/h [15].

$$Mg_2Si + 4HCl \rightarrow SiH_4 + 2MgCl_2 \Delta^\circ G_{40^\circ C} = -677\text{kJ} \quad (14)$$

$$Mg_2Si + 4HCl + 2H_2O \rightarrow 2MgCl_2 + SiO_2 + 4H_2 \Delta^\circ G_{40^\circ C} = -1119\text{kJ} \quad (15)$$

Table 4 Silane distribution obtained by GC–MS

Sample	Setup	Temperature (°C)	Concentration of acid (%)	Silane distribution (wt%)		
				SiH_4	Si_2H_6	Si_3H_8
Commercial Mg_2Si	Setup 1	40	12	58	28	14
MR-800		40	12	57	25	18
Commercial Mg_2Si	Setup 2	40	12	59	25	16
		40				
MR-800		40	12	61	27	12
MR-900		40	12	61 ± 1	25 ± 1	14 ± 1
MR-1100		40	12	62 ± 1	25 ± 0.4	13 ± 2
Commercial Mg_2Si		52	12	60	26	14
Commercial Mg_2Si		20	12	62	28	10
Commercial Mg_2Si		40	16	59	27	15

$$Mg_2Si + 2H_2O \rightarrow \begin{matrix} HO-Mg \\ HO-Mg \end{matrix} > SiH_2 \quad (16)$$

$$\begin{matrix} HO-Mg \\ HO-Mg \end{matrix} > SiH_2 + 4HCl \rightarrow -SiH_2 - +2MgCl_2 + 2H_2O + H_2 \quad (17)$$

$$-SiH_2 - +2H_2O \rightarrow SiO_2 + 2H_2 \quad (18)$$

$$-SiH_2SiH_2 - +H_2O \rightarrow SiH_2O + SiH_4 \quad (19)$$

$$-SiH_2SiH_2SiH_2 - +H_2O \rightarrow SiH_2O + Si_2H_6 \quad (20)$$

$$-SiH_2SiH_2SiH_2SiH_2 - +H_2O \rightarrow SiH_2O + Si_3H_8 \quad (21)$$

$$SiH_2O + 2H_2O \rightarrow SiO_2 + 3H_2 \quad (22)$$

Zhu et al. proposed a shrinking model to describe the reaction between silicide compounds and HCl acid solution [38]. They suggested that two layers are formed around a reacting particle: a product layer containing gas bubbles and a solid by-product and a gas–liquid film containing coalescence gas bubbles. Both these layers limit the acid diffusion toward the unreacted Mg_2Si particle center where the diffusion of HCl acid can be considered the rate limiting step. It is worth mentioning that stirring was employed to ensure adequate mixing of the reactants and to facilitate the elimination of the mentioned layers around partly reacted Mg_2Si particles. Using setup 2, Mg_2Si particles, which were dispersed in the water, led to a higher degree of silane formation at the early stage of reaction, as discussed previously [39]. The reaction commenced instantly after Mg_2Si and acid solution came into contact. As seen in Fig. 8, the temperature reached a maximum, also indicating that peak reaction occurred at the beginning of the reaction period. After the initial reaction, the rate of heat dissipation to the environment is higher than the released heat and hence, the temperature decreased toward the set reaction temperature. The pressure of the system exhibits a similar trend. The pressure increased abruptly at the beginning of the reaction and then declined to the set pressure of 1.3 bar using a pressure regulator which implies high amount of gas formation.

Outlook on a Process

Based on the results obtained in this work, the Union Carbide method as the industrial process and the Mg_2Si hydrolysis method are compared to provide an overview of their advantages and disadvantages as follows:

- In the current magnesiothermic process, SiO_2 reduction is carried out without direct CO_2 emissions. It may be argued that the present predominant method of producing primary Mg as a reductant (the Pidgeon process) is far from carbon free. However, recovery of Mg through chloride electrolysis of $MgCl_2$ (the established DOW process), recovered from the solution may provide a viable path to low carbon silane production, using green electricity.
- It was shown in our previous work that the exothermic magnesiothermic reduction of SiO_2 to produce Mg_2Si may be carried out with a reasonable reaction rate at 1000 °C, which is lower than the temperature required for carbothermic reduction of SiO_2, > 1800 °C, permitting a less energy consuming reduction process. The SiH_4 is also formed at a low temperature in the one-stage process of Mg_2Si hydrolysis in contrast to the Union Carbide method, where first Si and HCl reacts to form $SiHCl_3$, which is subsequently converted to SiH_4 through a redistribution process. The former stage is high temperature processes. In the Mg_2Si hydrolysis method, recovery of Mg is the main energy consuming step.
- During conversion of $SiHCl_3$ to SiH_4 in the Union Carbide method, three moles of $SiCl_4$ form per mole of SiH_4 formed theoretically. Therefore, it is necessary to recover $SiCl_4$ to have an efficient process. It is shown in this study that a SiH_4 yield of 21% can be achieved from hydrolysis of Mg_2Si, which is comparable with the SiH_4 yield of the industrial redistribution process. On the negative side, the by-products are SiO_2 (in the precipitate) and $SiCl_4$ for hydrolysis of Mg_2Si and the industrial redistribution process, respectively. Recovery of $SiCl_4$ is less energy intensive than recovery of SiO_2 and hence, the mass and energy balances for the two processes have to be compared and evaluated in-depth.

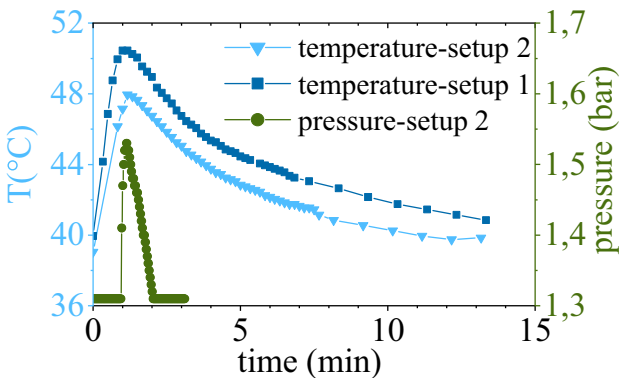

Fig. 8 Temperature of the acid solution and pressure inside the reactor over reaction time

Conclusions

In the current work, silane production through hydrolysis of Mg_2Si in HCl acid solution was investigated as an alternative silane production process. Magnesium silicide hydrolysis is attractive and straightforward method, where Mg_2Si can be produced through magnesiothermic reduction of quartz without direct greenhouse gas emissions. More details on the silane formation were provided under different reaction conditions such as temperature, reaction time, acid concentration, different Mg_2Si sources, different experimental setups, and relative amounts of reactants. The main conclusions of the present work can be summarized as follows:

- A solution temperature higher than 40 °C and acid concentration of 12% led to the total highest silane yield.
- The total silane yield (sum of Si in different silanes) obtained was 29% using the KOH solution analysis method. The measured silane yield was a few percent higher, about 32% using direct GC–MS gas analysis, demonstrating some yield improvement in comparison to previous studies, particularly for the SiH_4 yield. The Si contained in the original Mg_2Si was converted to silane and amorphous SiO_2 found in the solution residues after reaction. The mass fraction of Si entering the system found in silane corresponded to approximately 32%, while the residue contained approximately 68% of the silicon.
- The analyses of the produced silane gases show no significant differences between a commercial Mg_2Si source and a magnesiothermic product mixture of Mg_2Si and MgO.

Supplementary Information The online version contains supplementary material available at https://doi.org/10.1007/s40831-024-00817-2.

Funding Open access funding provided by NTNU Norwegian University of Science and Technology (incl St. Olavs Hospital - Trondheim University Hospital). This research was funded by Research Centre for Sustainable Solar Cell Technology (FME SuSolTech) co-sponsored by the Norwegian Research Council and industry partners, grant by number Project Number 257639. Infrastructure investment support for the GC–MS instrument provided by the FOR-INFRA programme of the Research Council of Norway under Project No. 245744.

Declarations

Conflict of interest The authors declare that they have no conflict of interest.

References

1. International Energy Agency (2022) Renewables 2022, analysis and forecast to 2027. https://www.iea.org/reports/renewables-2022
2. International Energy Agency (2022) Special report on solar PV global supply chains. https://www.iea.org/reports/solar-pv-global-supply-chains
3. International Energy Agency (2022) Trends in photovoltaic applications, IEA PVPS Task 1. https://iea-pvps.org/trends_reports/trends-2022/
4. Yang D (2019) Part I: polycrystalline silicon. In: Handbook of photovoltaic silicon. Springer-Verlag GmbH Germany, pp 7–126
5. International Technology Roadmap for Photovoltaic (ITRPV). 9th Edn. 2018. https://www.itrpv.net/
6. RECSilICON. https://recsilicon.com/technology/
7. Tangstad M (2013) Silicon in solar cells. In: Metal production in Norway. Academia Publishing, pp 121–155
8. Coleman LM (1982) Process for the production of ultrahigh purity silane with recycle from separation columns. US 4,340,574
9. Hesse K, Pätzold U (2006) Survey over the TCS process. In: Proceedings of the silicon for the chemical industry VIII. pp 157–166
10. Ceccaroli B, Pizzini S (2012) Processes. In: Advanced silicon materials for photovoltaic applications. Wiley, Hoboken
11. Litteral CJ (1978) Disproportonation of chloroslane. US 4,113,845
12. Bakay CJ (1976) Process for making silane. US 3,968,199
13. Stock A, Somieski C (1916) Siliciumwasserstoffe. I. Die Aus Magnesiumsilicid Und Säuren Entstehenden Siliciumwasserstoffe. Ber Dtsch Chem Ges 49:111–157
14. Johnson WC, Hogness TR (1934) The preparation of hydrogen compounds of silicon. J Am Chem Soc 56:1252. https://doi.org/10.1021/ja01320a509
15. Belot D, Rade J-Y, Piffard J-F, Larquet C, Cornut P (1987) Process and the apparatus for the production of silicon hydrides. US 4,698,218
16. Nandi KC, Mukherjee D, Biswas AK, Acharya HN (1993) Optimization of acid concentration, temperature and particle size of magnesium silicide, obtained from rice husk, for the production of silanes. J Mater Sci Lett 12:1248–1250. https://doi.org/10.1007/BF00506325
17. Culbertson JB (1951) Method of producing silanes. US 2,551,571
18. Fehér F, Schinkitz D, Strack H (1971) Beiträge Zur Chemie Des Siliciums Und Germaniums. Darstellung von Rohsilan in Einem 1-l-Reaktor. Z Anorg Allg Chem 385:202–208
19. Fehér F, Schinkitz D, Schaaf J (1971) Ein Verfahren Zur Darstellung Höherer Silane. Z Anorg Allg Chem 383:303–313. https://doi.org/10.1002/zaac.19713830311
20. Finholt AE, Bond AC, Wilzbach KE, Schlesinger HI (1947) The preparation and some properties of hydrides of elements of the fourth group of the periodic system and of their organic derivatives. J Am Chem Soc 69:2692–2696. https://doi.org/10.1021/ja01203a041
21. Taylor PA (1988) Purification techniques and analytical methods for gaseous and metallic impurities in high-purity silane. J Cryst Growth 89:28–38. https://doi.org/10.1016/0022-0248(88)90068-1

22. Sundermeyer W (1963) Hydrogenation of halogen compounds of elements of groups III and IV of the periodic systems. US 3,078,218
23. Kuratomi T, Yatsurugi Y (1971) Process for production of monosilane (SiH_4) and germanium hydride (GeH_4). US 3,577,220
24. Mukashev BN, Abdullin KA, Tamendarov MF, Turmagambetov TS, Beketov BA, Page MR, Kline DM (2009) A metallurgical route to produce upgraded silicon and monosilane. Sol Energy Mater Sol Cells 93:1785–1791. https://doi.org/10.1016/j.solmat.2009.06.011
25. Tamendarov MF, Mukashev BN, Abdullin KA, Kulekeev ZA, Bekturganov NS, Beketov BA (2006) Methods of Production of Pure Silicon, WO 2006041271A1
26. Rasouli A, Herstad KE, Safarian J, Tranell G (2022) Magnesiothermic reduction of natural quartz. Metall Mater Trans B 53:2132–2142. https://doi.org/10.1007/s11663-022-02513-6
27. Rasouli A, Tsoutsouva M, Safarian J, Tranell G (2022) Kinetics of magnesiothermic reduction of natural quartz. Materials (Basel) 15:6535. https://doi.org/10.3390/ma15196535
28. Arkles B (1997) Silanes. In: Kirk-Othmer encyclopedia of chemical technology, vol 22. Wiley, Hoboken, pp 38–69
29. Wyller GM (2019) Experimental investigation of monosilane pyrolysis. University of Oslo, Oslo
30. Stock A (1933) Hydrides of boron and silicon. Cornell University Press, Ithaca
31. Fehér F, Freund R (1973) Contributions to the chemistry of silicon and germanium, XXII (1) new silanes, bromosilanes and phenylsilanes. Inorg Nucl Chem Lett 9:937–940. https://doi.org/10.1016/0020-1650(73)80130-8
32. Fehér F, Hädicke P, Frings H (1973) Beiträge Zur Chemie Des Siliciums Und Germaniums, XXIII (1) Physikalisch-Chemische Eigenschaften Der Silane von Trisilan Bis Heptasilan. Inorg Nucl Chem Lett 9:931–936. https://doi.org/10.1016/0020-1650(73)80129-1
33. Wiberg E, Amberger E (1971) Hydrides of the elements of main groups I–IV. Elsevier Publishing Company, Amsterdam
34. Johnson WC, Isenberg S (1935) Hydrogen compounds of silicon. I. The preparation of mono- and disilane. J Am Chem Soc 57:1349–1353. https://doi.org/10.1021/ja01310a053
35. Serikkanov A, Shongalova A, Zholdybayev K, Tokmoldin N, Turmagambetov T, Pavlov A, Mukashev B (2022) Integration of Kazakhstan technologies for silicon and monosilane production with the suitable world practices for the production of solar cells and panels. Processes 10:1303. https://doi.org/10.3390/pr10071303
36. Schwarz R, Konrad E (1922) Über Den Reaktionsmechanismus Der Silan-Bildung Aus Magnesiumsilicid (I.). Ber Dtsch Chem Ges A B Ser 15:3242–3252
37. Fehér F, Tromm W (1955) Die Darstellung von Silanen Aus Magnesiumsilicid Und Hydrazoniumchlorid in Wasserfreiem Hydrazin. Z Anorg Allg Chem 282:29–40
38. Zhu M, Yue SY, Tang K, Safarian J (2020) New insights into silicon purification by alloying-leaching refining: a comparative study of Mg-Si, Ca-Si, and Ca-Mg-Si systems. ACS Sustain Chem Eng 8:15953–15966. https://doi.org/10.1021/acssuschemeng.0c05564
39. Khawam A, Flanagan DR (2006) Solid-state kinetic models: basics and mathematical fundamentals. J Phys Chem B 110:17315–17328. https://doi.org/10.1021/jp062746a